

# Signatures of the $\Delta$ isobar in spin observables of ${}^3\text{He}$ electrodisintegration

A. Deltuva

*Institute of Theoretical Physics and Astronomy, Vilnius University, Saulėtekio al. 3, LT-10257 Vilnius, Lithuania*

---

## Abstract

The electrodisintegration of  ${}^3\text{He}$  is considered focusing on the effects of the  $\Delta$  isobar excitation which is treated dynamically on the same footing as nucleons. In the region beyond the quasi-elastic peak the predicted transverse response functions  $R_T$  and  $R_{T'}$  are visibly affected. This leads to sizable  $\Delta$  isobar effects for inclusive and exclusive electron polarization asymmetries in particular kinematic regions. A measurement performed in the proposed regime could provide judgment for models of nuclear forces and currents.

*Key words:* Inelastic electron scattering, few-nucleon dynamics,  $\Delta$  isobar excitation, polarization asymmetry

---

## 1. Introduction

The  $\Delta$  isobar plays an important role in the nuclear dynamics. It manifests itself most prominently as the  $P$ -wave pion-nucleon resonance in the spin-isospin  $\frac{3}{2}$  channel around the total energy of 1232 MeV. In the intermediate energy regime the  $\Delta$  isobar is a dominant mechanism for the pion production and absorption in hadronic and electromagnetic processes [1]. However, even at considerably lower energies virtual excitations of nucleons ( $N$ ) to  $\Delta$  isobars yield important contributions to nuclear forces and electroweak currents. One of the most famous examples is the Fujita-Miyazawa three-nucleon force [2]. The majority of works describing the processes in systems with three or more nucleons relied on the static approximation for the  $\Delta$  isobar, that is, restricting the Hilbert space to purely nucleonic degrees of freedom while accounting for leading  $\Delta$  isobar contributions via effective nucleonic forces and current operators [3–5]. This simplifies the description of the few-nucleon problem but is not always reliable with respect to the  $\Delta$  isobar effect [6]. In contrast, the Hannover group pursued an alternative description where the  $\Delta$  isobar was an active degree of freedom treated on the same footing as nucleons [6–9]. This leads to a more complicated Hilbert space with the channel coupling, but avoids the static approximation and offers the possibility to include more rich dynamics in terms of  $\Delta$  isobar contributions, such as those mediated by heavier mesons.

Reactions in the three-nucleon system at energies below or around the pion-production threshold have been described considering the  $\Delta$  isobar as a stable baryon of spin and isospin  $\frac{3}{2}$ , since in this energy regime only a virtual excitation of a nucleon to a  $\Delta$  isobar is possible. Prominent  $\Delta$  isobar effects have been found in the differential cross section and some spin observables of the nucleon-deuteron elastic scattering and breakup and radiative capture [10,11]. Compared to those reactions, the electrodisintegration of the trinucleon bound state offers in addition the opportunity to test the models for the electromagnetic current at higher four-momentum transfers. However, the study of [12] found only small  $\Delta$  isobar effects in response functions and asymmetries of the inclusive  ${}^3\text{He}(e, e')$  reaction around the quasi-elastic peak. This result is consistent with Ref. [5], based on the  $\Delta$  isobar inclusion in the impulse approximation, as well as with a generally observed rather low sensitivity of those observables to the dynamics beyond the standard forces and currents [13]. An example for a sizable and beneficial  $\Delta$  isobar effect in the  ${}^3\text{He}(e, e')$  reaction is the transverse response function at large three-momentum transfer  $Q \sim 900$  MeV but low energy transfer  $Q_0$  close to the disintegration threshold [12]. Under those conditions the cross section and response functions are very small, rendering the measurement highly challenging. Furthermore, a large value of the three-momentum transfer suggests that relativistic corrections to the current are not negligible [14]. Thus, it would be desirable to explore the  $\Delta$  isobar effect in the region of lower  $Q$  values. Given the recent and ongoing efforts to study the spin structure of  ${}^3\text{He}$ , and thereby also of the neutron [15,16], the spin observables

---

*Email address:* arnoldas.deltuva@tfai.vu.lt (A. Deltuva).

in the  ${}^3\text{He}$  electrodisintegration are of a special interest.

Currently the most advanced and quantitative approach to interactions between nucleons and with electromagnetic probes is the chiral effective field theory. Its extensions including the  $\Delta$  isobar are in progress as well, however, the  $\Delta$  isobar most often is not yet considered as an active degree of freedom on the same footing as nucleons, i.e., the derived forces are purely nucleonic. Few attempts to overcome this restriction [17] are limited to rather low orders of the chiral expansion. Therefore the present study relies on a meson-theoretical but quantitatively most accurate model for the two-baryon potential with the  $\Delta$  isobar excitation [10], called CD Bonn +  $\Delta$ , and the associated model for the electromagnetic current [11,12], containing contributions due to the exchange of  $\pi$ ,  $\rho$ , and  $\omega$  mesons. In the three-nucleon system this leads to effective and mutually consistent three-nucleon forces and currents. The calculations using the purely nucleonic CD Bonn potential are used as reference to isolate the  $\Delta$  isobar effect.

Section II shortly recalls the calculation scheme, Sec. III presents the selected results for the electrodisintegration of  ${}^3\text{He}$ , and Sec. IV summarizes the work. Natural units  $\hbar = c = 1$  are used throughout the paper.

## 2. Calculation scheme

As customary, the electromagnetic interaction between the electron and the  ${}^3\text{He}$  nucleus is treated in the one-photon exchange approximation. The virtual photon couples to the nuclear electromagnetic current, whose operators are of one-baryon and meson-exchange two-baryon nature, both purely nucleonic and with the  $\Delta$  isobar excitation. They are schematically represented in Figs. 1 - 3 with explicit expressions given in the appendix of Ref. [11]. Full initial- and final-state interactions for nuclear states are included following the Faddeev theory [18,19] in a more general case with channel coupling. Instead of calculating separately a large number of final states it is convenient to solve Faddeev-type equations for auxiliary states

$$|X^\lambda\rangle = (1 + P)(J \cdot \epsilon^\lambda)|B\rangle + PTG_0|X^\lambda\rangle, \quad (1)$$

where  $|B\rangle$  denotes the initial  ${}^3\text{He}$  bound state,  $J$  is the four-component electromagnetic current operator,  $\epsilon^\lambda$  is the four-dimensional vector of the virtual photon polarization denoted by  $\lambda$ ,  $G_0$  is the free resolvent,  $T$  is the coupled-channel two-baryon transition matrix, and  $P$  is the sum of two cyclic permutation operators; see Refs. [11,12] for more details. The auxiliary states include the action of the electromagnetic current on  ${}^3\text{He}$  bound state and all final-state interactions in the three-nucleon continuum. Consequently, their projection to nucleon-deuteron or three-nucleon channel states (that are simply free waves) yields reaction amplitudes and thereby all observables of two- and three-cluster electrodisintegration of  ${}^3\text{He}$  as well as response functions [11,12].

Equations (1) are solved in the momentum-space partial-wave representation, including both total isospin  $\frac{1}{2}$  and  $\frac{3}{2}$

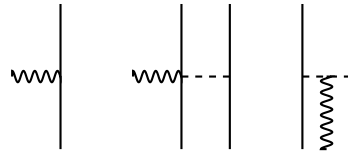


Fig. 1. Purely nucleonic one- and two-baryon electromagnetic currents. Thin solid line denotes the nucleon, the wavy line denotes the photon, the dashed line denotes the instantaneous meson ( $\pi, \rho, \omega$ ) exchange.



Fig. 2. One- and two-baryon electromagnetic currents with the excitation of the  $\Delta$  isobar, that is denoted by a thick line. Hermitean-adjoint contributions are taken into account as well.



Fig. 3. One- and two-baryon electromagnetic currents connecting states with a  $\Delta$  isobar. Due to their negligibly small contributions heavier mesons ( $\rho, \omega$ ) are not included.

components as well as sufficiently high angular momenta such that the results are well converged; for example, the total angular momentum up to  $\frac{35}{2}$  is taken into account. The states  $|X^\lambda\rangle$  have components in all basis states, that is, in the considered momentum-space partial-wave representation they depend on two continuous variables, the Jacobi momenta for the relative motion of three particles, and have  $NNN$  and  $NN\Delta$  components with a large number of orbital angular momentum, spin, and isospin channels, compatible with the given total angular momentum and parity. An important conceptual improvement as compared to Ref. [12] is the inclusion of the Coulomb interaction between charged baryons using the method of screening and renormalization [20], though the results for inclusive observables are barely affected, except at very low excitation energies near the threshold.

## 3. Results

Response functions and asymmetries for the  ${}^3\text{He}(e, e')$  process with the dynamic  $\Delta$  isobar excitation have been calculated in Refs. [12,20] for a limited number of kinematic situations; no significant  $\Delta$  isobar effects have been established except for the near-threshold transverse response function at high three-momentum transfer. The results of Refs. [12,20] remain valid and are not repeated here. One of the shortcomings in those calculations is the displacement

of the quasi-elastic peak as compared to the experimental data. It is observed also in other works [13,21] that use non-relativistic kinematics and dynamics for the three-nucleon system, since the quasi-elastic scattering conditions calculated with relativistic and nonrelativistic kinematics deviate from each other with increasing momentum transfer. Several approaches have been proposed to correct this shortcoming, such as the use of the active-nucleon Breit frame and the two-fragment model [21]. The present work proposes a simple prescription based on relativistic

$$\psi_r(Q_0, Q) = (\lambda - \tau) \left\{ \epsilon_F \left[ (1 + \lambda)\tau + \kappa \sqrt{\tau(1 + \tau)} \right] \right\}^{-1/2} \quad (2)$$

and nonrelativistic

$$\psi_{nr}(Q_0, Q) = \frac{m}{Qk_F} \left( Q_0 - \epsilon_B - \frac{Q^2}{2m} \right) \quad (3)$$

scaling variables taken from Refs. [22,23]. Here  $\lambda = (Q_0 - \epsilon_B)/2m$ ,  $\kappa = Q/2m$ ,  $\tau = (Q^2 - Q_0^2)/4m^2$ ,  $\epsilon_F = [1 + (k_F/m)^2]^{1/2} - 1$ , and  $m$  is the average nucleon mass. Parameters  $k_F$  and  $\epsilon_B$  have the meaning of the Fermi momentum and  $^3\text{He}$  binding energy, their values are chosen to be  $k_F = 180$  MeV and  $\epsilon_B = 7.72$  MeV, though the final results are not sensitive to small variations of  $k_F$  and  $\epsilon_B$ . The key point is that experimental and theoretical response functions peak very close to  $\psi_r(Q_0, Q) = 0$  and  $\psi_{nr}(Q_0, Q) = 0$ , respectively, though  $(Q_0, Q)$  values in both descriptions are not identical. Thus, it makes sense to compare the experimental data as a function of  $\psi_r$  with the nonrelativistic theoretical predictions as functions of  $\psi_{nr}$ . In other words, the experimental data at the given  $(Q_0, Q)$  value should be compared with theoretical predictions taken at slightly modified values  $(Q'_0, Q')$  satisfying  $\psi_r(Q_0, Q) = \psi_{nr}(Q'_0, Q')$ . Obviously, there is some arbitrariness in choosing two variables  $(Q'_0, Q')$  constrained by a single relation, an additional condition is needed. The present work uses  $Q' = Q$  though other choices are possible as well. I emphasize that this is not a rigorous treatment but a prescription that is physicswise meaningful in the vicinity of the quasi-elastic peak. It may be not appropriate near the disintegration threshold where the excitation energy is the relevant variable.

An example applying this prescription is presented in Fig. 4 for the transverse response function  $R_T$ ; it is chosen since it is more affected by the  $\Delta$  isobar than the longitudinal one.  $R_T$  is shown for the momentum transfer ranging from  $Q = 250$  to 550 MeV. At the highest  $Q$  value the results without the above-described correction for the relativistic kinematics are included for the comparison. The effect is sizable, the quasi-elastic peak is displaced by about 13 MeV in  $Q_0$ , and the account for the data beyond the peak fails. In contrast, with the proposed correction the description of the experimental data is good in the whole considered regime, especially given the fact that the two sets of data by Marchand et al. [24] and Dow et al. [25] are in variance as well; theoretical predictions favor the latter set. The  $\Delta$  isobar effect is insignificant around the quasi-elastic

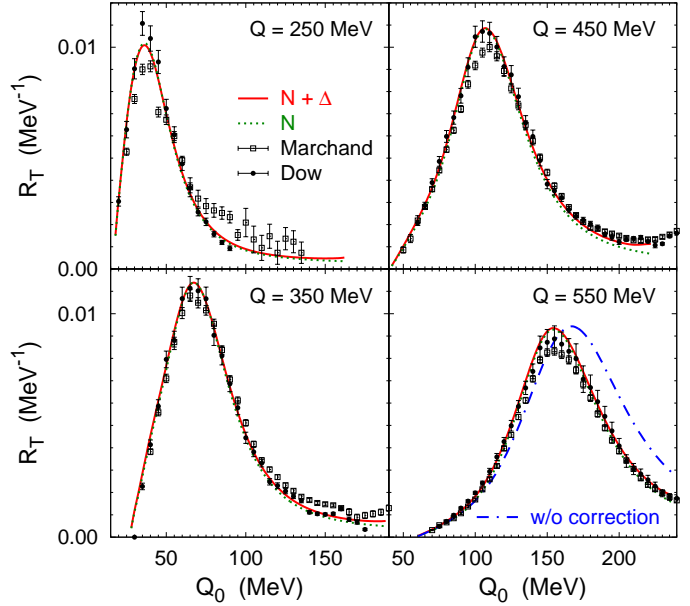


Fig. 4. (Color online) Transverse response function  $R_T$  as a function of the energy transfer  $Q_0$  for momentum transfer values  $Q = 250, 350, 450,$  and  $550$  MeV. Results with and without the  $\Delta$  isobar excitation are shown by solid and dotted curves, respectively. The dashed-dotted curve at  $Q = 550$  MeV displays predictions including the  $\Delta$  isobar but without the correction for relativistic kinematics. The experimental data are from Refs. [24] ( $\square$ ) and [25] ( $\bullet$ ).

peak but is more pronounced at larger values of the energy transfer beyond the peak, most evident at  $Q = 450$  MeV; it is clearly supported by the data. This is consistent with the results for hadronic scattering [10] where the  $\Delta$  isobar effect is also enhanced at higher energies. The calculations are not pushed to even higher energies for the reason that the underlying potentials are not fitted to the two-nucleon data at those higher energies. The present results are therefore limited to the total relative three-nucleon energy below 175 MeV, well below the theoretical  $\Delta$  isobar production threshold of 293 MeV.

The spin-dependent transverse and transverse-longitudinal response functions  $R_{T'}$  and  $R_{TL'}$  are studied to a lesser extent. The predictions for the same values of the momentum transfer are presented in Fig. 5. To match the convention used in other works, e.g., Ref. [13], the results in the convention of Ref. [12] are multiplied by  $-1$  and  $-\frac{1}{2}$  for  $R_{T'}$  and  $R_{TL'}$ , respectively. The results confirm rapid changes in the shape of  $R_{TL'}$  observed in Ref. [13]. The  $\Delta$  isobar effect appears to be quite insignificant, except for  $R_{T'}$  near the quasi-elastic peak and at larger values of the energy transfer beyond the quasi-elastic peak, i.e., the regime with a visible effect also in  $R_T$ .

Response functions  $R_{T'}$  and  $R_{TL'}$  determine the electron polarization asymmetries for the inclusive  $^3\text{He}(e, e')$  processes [26]. Calculations for few existing measurements around or below the quasi-elastic peak [27,28] do not exhibit significant sensitivity to the three-nucleon force [13] or  $\Delta$  isobar [12]. The question is under what conditions the  $\Delta$  isobar effects shown in previous figures would show up in

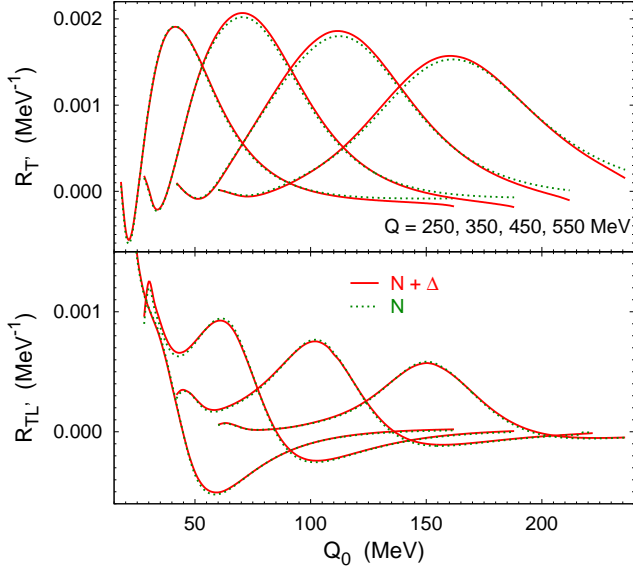


Fig. 5. (Color online) Transverse and transverse-longitudinal response functions  $R_T$  and  $R_{TL}$  as functions of the energy transfer  $Q_0$ . Four sets of curves from left to right correspond to momentum transfer values  $Q = 250, 350, 450,$  and  $550$  MeV. Curves are as in Fig. 4.

the asymmetries that are measurable observables. From the general asymmetry dependence on the electron kinematics [26] it is obvious that the electron scattering angles  $\theta_e$  should take moderate or large values, otherwise the asymmetries will be small, just few percent as in Refs. [27,28]. Furthermore, to probe the kinematic region around  $Q \sim 400$  MeV,  $Q_0 \sim 200$  MeV with not too small  $\theta_e$  the electron beam energy  $E_i$  should be of few hundred MeV, not in the GeV region. Few examples of the electron asymmetry predictions under such conditions are presented in Fig. 6, assuming 350 MeV electron energy, spin of the  ${}^3\text{He}$  target oriented in the beam direction, and five different electron scattering angles ranging from 30 to 150 degrees. The end points of the five sets of curves in Fig. 6 correspond to rather moderate values of  $Q = 210, 303, 377, 431,$  and  $462$  MeV, the total energies being around or slightly above the pion threshold. The asymmetry may become as large as 20% while at larger energy transfers the inclusion of the  $\Delta$  isobar changes it by about 10% on the absolute scale, e.g., from 7% to 17% at  $\theta_e = 90$  deg and from -5% to 6% at  $\theta_e = 150$  deg. The shown observable is dominated by the  $R_{T'}$  contribution which together with  $R_T$  is most affected by the  $\Delta$  isobar. Their absolute values well beyond the quasi-elastic peak are small, but on a relative scale the  $\Delta$  isobar effect is important. A more detailed analysis reveals that the effect is dominated by the single-baryon current with  $\Delta$  isobar excitation, but  $R_{T'}$  gets visible contribution also from two-baryon meson-exchange currents with  $\Delta$  isobar excitation. Of course,  $NN\Delta$  components in the initial bound and final scattering states are necessary for the inclusion of those currents, they are generated dynamically by the coupled-channel potential. Note that for the perpendicular orientation of the target spin with respect to the beam di-

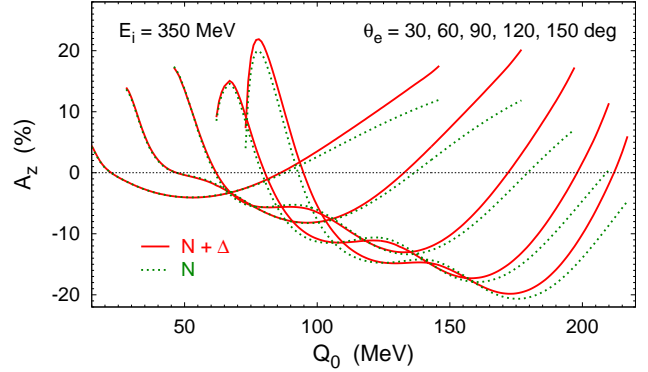


Fig. 6. (Color online) The electron polarization asymmetry for the  ${}^3\text{He}$  spin oriented parallel to the electron beam as a function of the energy transfer  $Q_0$ . The electron energy is 350 MeV, five sets of curves from left to right correspond to electron scattering angles  $\theta_e = 30, 60, 90, 120,$  and  $150$  deg. Curves are as in Fig. 4.

rection the effects are less pronounced, due to the reduced relative weight of  $R_{T'}$  and increased weight of  $R_{TL}$ .

For the experimental measurement of the asymmetry and the verification of the effect the absolute values of the cross section are important. Obviously they are considerably lower than in the vicinity of the quasi-elastic peak. In the region of interest  $Q_0 \geq 130$  MeV in Fig. 6 the differential cross section decreases with increasing  $Q_0$  and ranges roughly from 1500 to 60 pb/(MeV sr), with a moderate dependence on the angle. Obviously this is lower by several orders of magnitude as compared to the vicinity of the quasi-elastic peak. On the other hand, it is still higher by several orders of magnitude than in the near-threshold measurement [29] that reported values as small as 10 fb/(MeV sr).

Given the sizable  $\Delta$  isobar effect for the inclusive asymmetry, one may expect even larger effects in exclusive kinematics. An example for the  ${}^3\text{He}(e, e'd)$  reaction in coplanar kinematics is presented in Fig. 7, the total energy is slightly below the pion threshold. In particular regions of the laboratory deuteron emission angle  $\Theta_d$  the  $\Delta$  isobar effect is significant, both for the differential cross section and the asymmetry. The challenge in the experimental verification again would be low values of the cross section. On the other hand, the experiment reported in Ref. [30] measured the differential cross section values below 10 pb/(MeV sr<sup>2</sup>). Thus, the measurement of the  ${}^3\text{He}$  two-cluster electrodisintegration in the kinematics of Fig. 7 might be viable. The exclusive three-cluster breakup requires the detection of three-particles with even lower cross section and is even more challenging.

As for the inclusive observables in Figs. 4 - 6, the  $\Delta$ -isobar effect is largely dominated by the single-baryon current with the magnetic dipole  $\Delta$ -isobar excitation, the first diagram in Fig. 2. The respective form factor  $g_{\Delta N}^{M1}(q^2)$  where  $q^2 = Q^2 - Q_0^2$  is taken over from Ref. [12] with  $g_{\Delta N}^{M1}(0) = 4.59$  in units of nuclear magneton. Fits to the experimental data using different dynamical models [1] yield  $g_{\Delta N}^{M1}(0)$  values ranging from 4.52 to 4.61, while 4.71 was employed in Ref. [31]. Thus, even taking into account uncertainties in

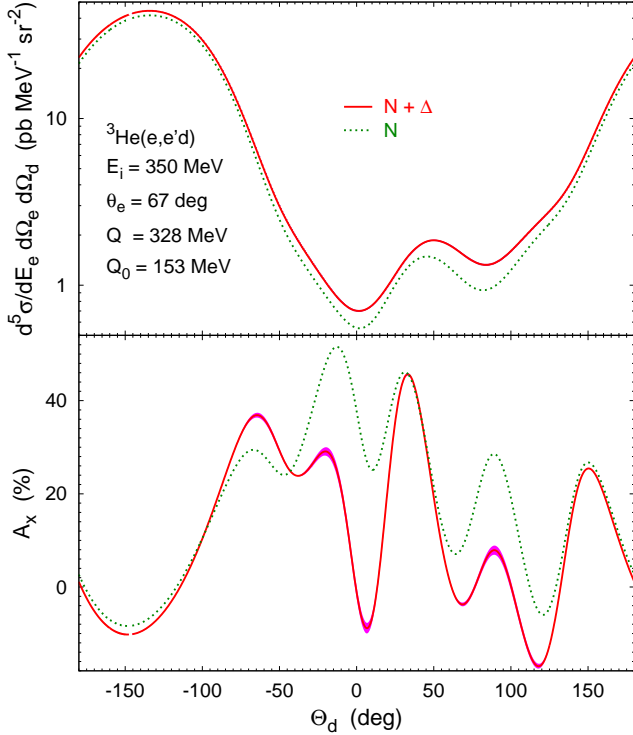


Fig. 7. (Color online) The differential cross section and electron polarization asymmetry for the  ${}^3\text{He}$  spin in the scattering plane oriented perpendicular to the electron beam as functions of the deuteron emission angle  $\Theta_d$ . Kinematics conditions are specified in the plot. Curves are as in Fig. 4. The shaded area reflects the 5% uncertainty in the magnetic dipole form factor  $g_{\Delta N}^{M1}(q^2)$ .

the  $q^2$ -dependence, the overall uncertainty of the presently used  $g_{\Delta N}^{M1}(q^2)$  should not exceed 5%. The resulting uncertainty for the  ${}^3\text{He}(e, e'd)$  reaction observables in Fig. 7 is represented by the shaded area around the solid curve and obviously does not change previous conclusions.

#### 4. Summary

The electrodisintegration of the  ${}^3\text{He}$  nucleus was considered focusing on the effects of the  $\Delta$  isobar excitation in electron polarization asymmetries. The  $\Delta$  isobar was treated dynamically in electromagnetic currents and initial and final hadronic states. Three-particle equations of the rigorous nonrelativistic Faddeev theory were solved in the momentum-space representation leading to well-converged results.

The correction for the relativistic kinematics using a simple prescription based on the relativistic and nonrelativistic scaling variables places the quasi-elastic peak in the right position and provides a good description of the experimental data. The region of the quasi-elastic peak is barely affected by the inclusion of the  $\Delta$  isobar but for larger energy transfer values both transverse response functions  $R_T$  and  $R_{T'}$  show visible effects, in contrast to longitudinal and longitudinal-transverse ones. The consequences are predicted sizable  $\Delta$  isobar effects for inclusive electron

asymmetries in particular kinematic regions, typically for few hundred MeV electron beams, moderate to large electron scattering angles, and energy transfer values around 150 or 200 MeV. The effects appear even more spectacular for observables of exclusive processes such as  ${}^3\text{He}(e, e'd)$ . The experiment performed under similar conditions could provide judgment for models of nuclear forces and currents, especially regarding the treatment of the  $\Delta$  isobar.

#### References

- [1] V. Pascalutsa, M. Vanderhaeghen, S. N. Yang, *Physics Reports* 437 (2007) 125.
- [2] J. Fujita, H. Miyazawa, *Prog. Theor. Phys.* 17 (1957) 360.
- [3] J. Carlson, R. Schiavilla, *Rev. Mod. Phys.* 70 (1998) 743.
- [4] L. E. Marcucci, M. Viviani, R. Schiavilla, A. Kievsky, S. Rosati, *Phys. Rev. C* 72 (2005) 014001.
- [5] L. Yuan, W. Leidemann, V. D. Efros, G. Orlandini, E. L. Tomusiak, *Physics Letters B* 706 (2011) 90.
- [6] P. U. Sauer, *Prog. Part. Nucl. Phys.* 16 (1986) 35.
- [7] C. Hajduk, P. U. Sauer, *Nucl. Phys. A* 322 (1979) 329.
- [8] C. Hajduk, P. U. Sauer, W. Struerve, *Nucl. Phys. A* 405 (1983) 581.
- [9] S. Nemoto, K. Chmielewski, J. Haidenbauer, U. Meyer, S. Oryu, P. U. Sauer, *Few-Body Systems* 24 (1998) 241.
- [10] A. Deltuva, R. Machleidt, P. U. Sauer, *Phys. Rev. C* 68 (2003) 024005.
- [11] A. Deltuva, L. P. Yuan, J. Adam Jr., A. C. Fonseca, P. U. Sauer, *Phys. Rev. C* 69 (2004) 034004.
- [12] A. Deltuva, L. P. Yuan, J. Adam Jr., P. U. Sauer, *Phys. Rev. C* 70 (2004) 034004.
- [13] J. Golak, R. Skibiński, H. Witała, W. Glöckle, A. Nogga, H. Kamada, *Phys. Rep.* 415 (2005) 89.
- [14] L. Yuan, V. D. Efros, W. Leidemann, E. L. Tomusiak, *Phys. Rev. C* 82 (2010) 054003.
- [15] M. Mihovilović, *et al.*, *Phys. Rev. Lett.* 113 (2014) 232505.
- [16] V. Sulkosky *et al.*, *Nature Physics* 17 (2021) 687.
- [17] S. Strohmeier, N. Kaiser, *Nucl. Phys. A* 1002 (2020) 121980.
- [18] L. D. Faddeev, *Zh. Eksp. Teor. Fiz.* 39 (1960) 1459 [*Sov. Phys. JETP* 12, 1014 (1961)].
- [19] E. O. Alt, P. Grassberger, W. Sandhas, *Nucl. Phys. B* 2 (1967) 167.
- [20] A. Deltuva, A. C. Fonseca, P. U. Sauer, *Phys. Rev. C* 72 (2005) 054004.
- [21] V. D. Efros, W. Leidemann, G. Orlandini, E. L. Tomusiak, *Phys. Rev. C* 83 (2011) 057001.
- [22] W. M. Alberico, A. Molinari, T. W. Donnelly, E. L. Kronenberg, J. W. Van Orden, *Phys. Rev. C* 38 (1988) 1801.
- [23] L. Andreoli, J. Carlson, A. Lovato, S. Pastore, N. Rocco, R. B. Wiringa, *Phys. Rev. C* 105 (2022) 014002.
- [24] C. Marchand *et al.*, *Phys. Lett. B* 153 (1985) 29.
- [25] K. Dow *et al.*, *Phys. Rev. Lett.* 61 (1988) 1706.
- [26] T. W. Donnelly, A. S. Raskin, *Ann. Phys. (N.Y.)* 169 (1986) 247.
- [27] W. Xu *et al.*, *Phys. Rev. Lett.* 85 (2000) 2900.
- [28] F. Xiong *et al.*, *Phys. Rev. Lett.* 87 (2001) 242501.
- [29] R. S. Hicks *et al.*, *Phys. Rev. C* 67 (2003) 064004.
- [30] E. Jans *et al.*, *Nucl. Phys. A* 475 (1987) 687.
- [31] F. Ritz, H. Göller, T. Wilbois, H. Arenhövel, *Phys. Rev. C* 55 (1997) 2214.